Nuclear Engineering and Technology 56 (2024) 3276–3285

Contents lists available at ScienceDirect

Nuclear Engineering and Technology

journal homepage: www.elsevier.com/locate/net

Original Article

Development of uncertainty quantification module for VVER analysis in STREAM/RAST-V two-step method

Jaerim Jang [a], Yunki Jo [b], Deokjung Lee [b,c,*]

[a] Korea Atomic Energy Research Institute, Daedeok-daero 989-111, Yuseong-gu, Daejeon, 305-335, Republic of Korea
[b] Department of Nuclear Engineering, Ulsan National Institute of Science and Technology, 50 UNIST-gil, Eonyang-eup, Ulju-gun, Ulsan, 44919, Republic of Korea
[c] Advanced Nuclear Technology and Services, 406-21 Jonga-ro, Jung-gu, Ulsan, 44429, Republic of Korea

ARTICLE INFO

Keywords:
UAM benchmark
Stochastic sampling
Uncertainty quantification
Kozloduy-6
Two-step method

ABSTRACT

This paper introduces the creation of a module for Uncertainty Quantification (UQ) specifically designed for VVER analysis through the implementation of the STREAM/RAST-V two-step approach. The aim was to expand the range of use by developing a UQ module tailored for analyzing VVER. This research presents two innovative computational functionalities: (1) development of a library for the pin-based pointwise energy slowing down method (PSM), and (2) extension of the analysis area to study hexagonal-geometry fuel assemblies. The proposed UQ scheme was evaluated through verification using UAM benchmark, and comparative analysis between codes using SCALE 6.2.2 for. STREAM provides an accuracy comparable to that of SCALE 6.2.2. Additionally, a PSM covariance library was utilized in the calculations, achieving 0.7941% and 0.7907% accuracies in the hot full power and hot zero power calculations, respectively. To assess the UQ sequences in the two-step method, the STREAM/RAST-V calculation scheme was verified using the STREAM lattice code. To conclude, this study furnishes comprehensive insights into the development of the UQ module within the two-step method for VVER analysis, and it validates its performance through utilization of the UAM benchmark.

1. Introduction

This research elucidates the developed uncertainty quantification (UQ) module within the STREAM/RAST-V two-step methodology for VVER analysis. The UQ analysis approach has been expanded compared to previous studies [1,2] by introducing two key novel features in the UQ process: (1) generation of a pin-based pointwise energy slowing down method (PSM) covariance library [3], and (2) expansion of the application area to include hexagonal geometry fuel assembly (FA) analysis. To assess these novel features, several verifications were performed in this study, with SCALE 6.2.2, which was used for comparative analysis between codes, leveraging the variance-to-covariance matrix (VCM) of SCALE 6.2 [4]. Additionally, for comprehensive solutions, this study employs the VCM of ENDF/B-VII.1 [5].

UQ finds application across diverse domains such as licensing examination, design advancement, and safety analysis. For example, uncertainty is harnessed to establish safety criteria, such as the upper safety limit, in burnup credit assessments crucial for the design of storage systems for spent nuclear fuel [1]. In safety analysis with transient simulation (*e.g.*, rod ejection), the uncertainty arising from neutronic data and input parameters helps define the confidence range of the hot cell. Consequently, projects and benchmarks such as the Consortium for Advanced Simulation of Light Water Reactors [6] and UAM [7] have emerged. These initiatives aim to enhance the competitiveness of participating laboratories' code systems. In the UAM benchmark, the participation was extended to 19 codes and 15 countries [7]. To align with these trends, a UQ calculation module was developed in in-house two-step code [1,2]. This study elaborates on this module and validates its results using the UAM benchmark by comparing the outcomes with those from SCALE 6.2.2.

As established in previous studies [8,9], a module for analyzing hexagonal geometry FAs was integrated into our proprietary two-step code system, STREAM/RAST-V [10,11]. The computational capacity of this hexagonal geometry reactor has been thoroughly verified and validated with various benchmarks [8,9]. To provide preliminary UQ results with a hexagonal FA using STREAM/RAST-V, Kozloduy-6 from the UAM benchmark was utilized in this study [7].

As illustrated in a prior investigation [3], the PSM resonance

* Corresponding author. Department of Nuclear Engineering, Ulsan National Institute of Science and Technology, 50 UNIST-gil, Eonyang-eup, Ulju-gun, Ulsan, 44919, Republic of Korea.
E-mail address: deokjung@unist.ac.kr (D. Lee).

https://doi.org/10.1016/j.net.2024.03.028
Received 13 September 2023; Received in revised form 24 February 2024; Accepted 20 March 2024
Available online 21 March 2024

Table 1
List of reactions employed during perturbation involving 72-group (72G) VCM.

#	Reaction
1	Elastic scattering XS, (z, z0)
2	Inelastic scattering XS, (z, n)
3	Fission XS, (z, fission)
4	Capture XS, (z, γ)
5	Manufacture of two neutrons, (z, 2n)
6	Manufacture of three neutrons, (z, 3n)
7	Manufacture of a proton, (z,p)
8	Manufacture of a deuteron, (z, d)
9	Manufacture of a triton, (z, t)
10	Manufacture of an alpha particle, (z, α)
11	Manufacture of a triton and 2 alpha particles, (z, t2 α)
12	Mean quantity of prompt neutrons emitted per fission occurrence, $\bar{\nu}_p$
13	Mean quantity of delayed neutrons emitted per fission occurrence, $\bar{\nu}_d$
14	Fission spectrum, $f(E \rightarrow E')$

Table 2
Cross section type used in calculation (for PSM) with 10,000G VCM.

#	Reaction
1	Fission XS, (n, fission)
2	Capture XS, (z, γ)
3	Total XS, (z, t)

treatment yields more accurate results than the Calvik's two-term rational approximation (EQ) resonance treatment used in the prior UQ module [12–14]. Consequently, to broaden the scope of applications and provide more precise results, this study describes the development of a UQ module and libraries specifically designed for PSM resonance treatment.

The structure of this manuscript is outlined as follows: Section 2 furnishes an elaborate exposition of the computational methodology with resonance treatment and generation progress of a covariance library, and resonance treatment. To assess the developed covariance library and UQ module, the UAM benchmark was used for calculations. Section 3 contains the detailed benchmark specifications. Section 4 presents detailed UAM benchmark results and a comparison of the STREAM calculation capability with the covariance libraries for PSM and EQ [12–14].

2. Code system

This section deals with the details of STREAM/RAST-V two-step method for UQ. The perturbation of the cross sectional module was conducted using STREAM with covariance data. In the STREAM/RAST-V dual-stage methodology, STREAM generates a set of group constants using perturbed cross-sectional data, followed by the utilization of RAST-V for three-dimensional core simulation incorporating perturbed few-group cross sections (XSs) generated by STREAM. In the preceding iteration of the UQ module, resonance treatment was limited to the EQ method due to the absence of support from the PSM VCM. As demonstrated in previous studies [3], PSM offers more accurate results than the EQ method. Therefore, in order to improve the calculation capability of lattice code and broaden the scope of application for the created UQ module, a VCM and perturbation module tailored for PSM were formulated.

In addition, the updated version of NJOY-2016 [15] code is employed for the generation of a VCM for comparison with previous studies [1,2]. The EQ covariance library was constructed utilizing a 72-energy group structure encompassing 14 reactions listed in Table 1. In this study, VCM between difference isotopes are not considered such as VCM between ^{235}U (z, γ) and ^{238}U (z, γ). For the PSM covariance library, a 10,000-group structure was used for the resonance regions of the three reactions, as listed in Table 2. Details of resonance treatment

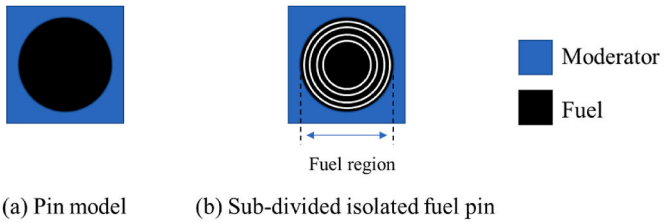

Fig. 1. Fuel pin model used in resonance treatment.

methods and perturbation methods are in Section 2.1 and 2.2, separately.

During the depletion calculation, STREAM leverages the CRAM method [10] to resolve the Bateman equation by computing 1640 isotopes [16]. Within the STREAM/RAST-V two-step methodology, RAST-V employs a micro depletion solver for approximately 36 isotopes [17]. Our in-house two-step code system has been rigorously tested and authenticated with a variety of benchmarks [9,18]. The rectangular-geometry FA analysis module has been validated using various core types, including OPR-1000, Westinghouse 3-loop, and APR-1400 [18]. As part of the continuing research, a hexagonal-geometry FA analysis module was developed to broaden the application scope, and its computational ability was tested and validated with various VVERs [8,9]: Rostov-II, AER-DYN-001, Kalinin-3, AER--DYN-002, X2, and Novovonezh-4. In order to expand the versatility of the UQ module, it was developed and validated for a hexagonal-geometry FA employing the UAM benchmark. Section 4 provides an elaborate exposition of the outcomes derived from this verification procedure.

2.1. Resonance treatment used in UQ

The primary distinction between the EQ and PSM methods lies in the use of pointwise cross sectional data for the resonance region. The EQ method utilizes 72 groups of cross sectional data in both the non-resonance and resonance regions. In contrast, PSM applies 72 group XS data for the non-resonance region, while employing 10,000 group (point-wise) XS data in the resonance region. Consequently, during the UQ with the EQ, a perturbation of the 72 group XS was performed. Simultaneously, during UQ with PSM, perturbations of both the 72 group XS and the 10,000 group XS were carried out.

The EQ is an equivalence theory with Carlvik's two-term rational approximation [19,20]. The foundational principle of this equivalence theory posits that the probability of neutron escape from resonance material can be approximated through a rational function correlating to the total cross section of a resonance nuclide. The expression for the escape cross section is articulated through an analytical formula, incorporating the shadowing effect via the Dancoff factor. The designation "2-term" pertains to the application of Carlvik's duo of terms in delineating the Dancoff factor, as elucidated in Equation (1) [20].

$$P_e = 2\frac{2\Sigma_e}{\Sigma_{t,F} + 2\Sigma_e} - \frac{3\Sigma_e}{\Sigma_{t,F} + 3\Sigma_e}, \tag{1}$$

where Σ_e represents the escape macroscopic cross section, and $\Sigma_{t,F}$ is the total macroscopic cross section in the fuel region. P_e denotes the fuel escape probability. The EQ method has the advantage of simplifying the definition of effective cross sectional data while still providing a reasonable solution. Subplot (a) of Fig. 1 was used for the EQ calculations.

The PSM's core concept involves the use of segmented fuel pins, as shown in subplot (b) of Fig. 1 [3]. Its methodology unfolds in three stages to estimate collision probabilities [3]: initially defining collision probability for subdivided fuel pins using the CPM solver, then determining the Dancoff factor with Carlvik's method and adjusting for

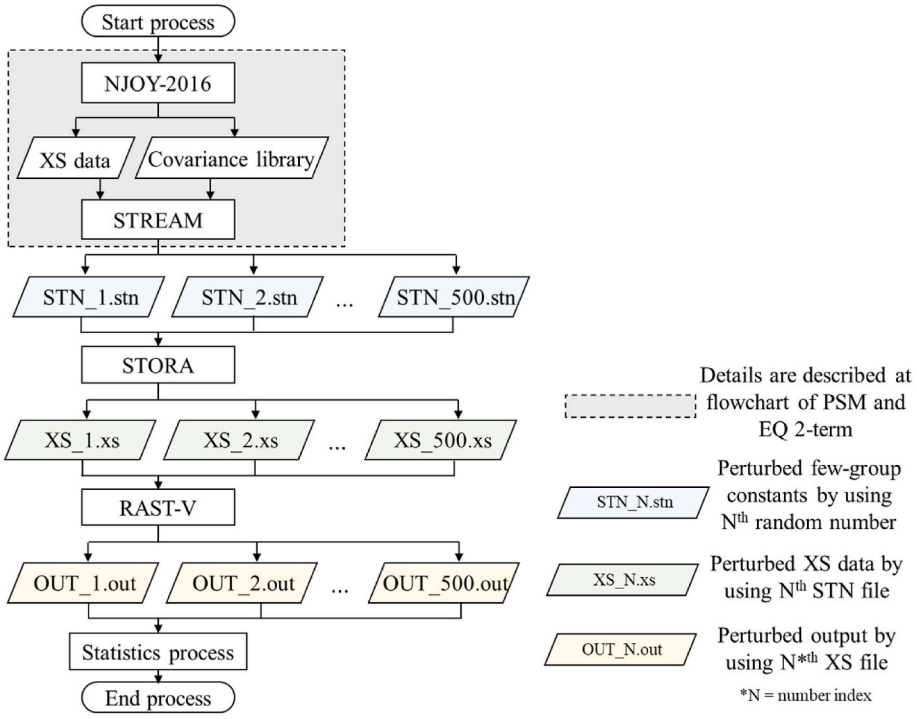

Fig. 2. Flowchart of perturbed cross section data in two-step method.

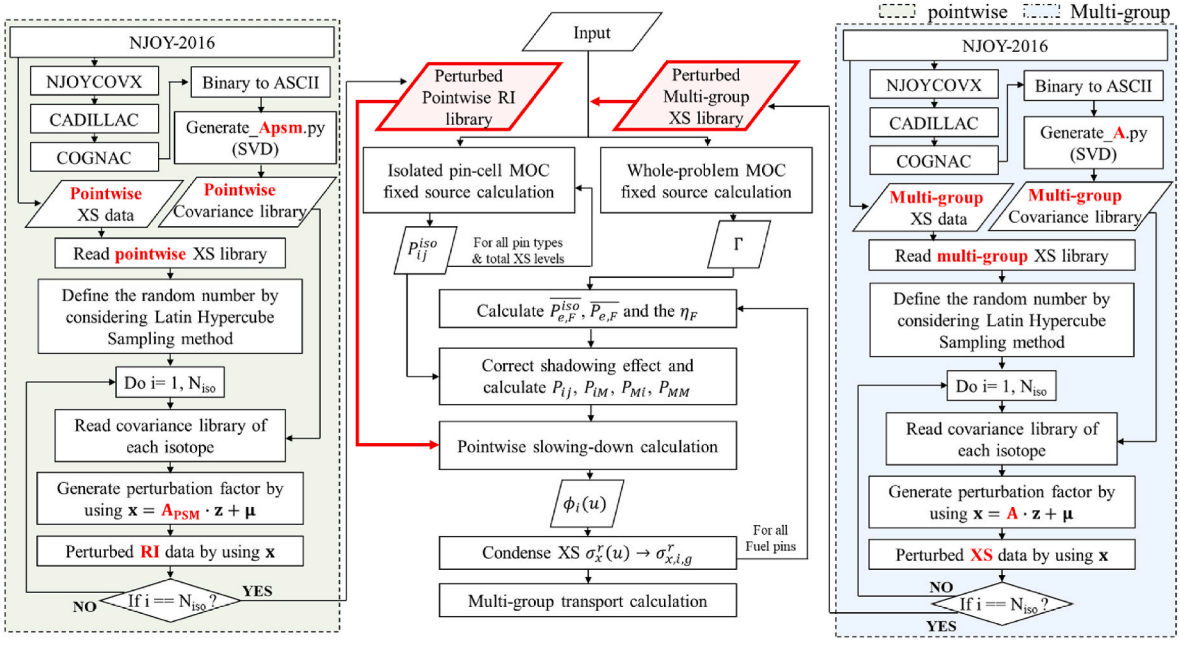

Fig. 3. Flowchart of perturbed XS based on PSM VCM.

shadowing effects to reconcile differences in fuel escape probabilities. Finally, it applies these corrections to refine both escape and collision probabilities.

2.2. Stochastic sampling method

RAST-V incorporates an UQ module developed based on the stochastic sampling method. This section outlines the calculation scheme for the stochastic sampling method and the covariance library used. Notably, only the explicit effect is considered when calculating the uncertainty owing to cross sectional data. To develop the UQ module, a stochastic sampling method based on reference [21] was used. As indicated in previous studies [1,2], the covariance matrix and singular value decomposition (SVD) methods were utilized to perturb neutronics data. In total, 182 isotopes were used for the calculations. The ENDF/B-VII.1 covariance data were generated using NJOY-2016 [15].

Fig. 2 illustrates a flowchart of the perturbed neutronics data. To elucidate the perturbation process in PSM and EQ calculations, detailed flowcharts are illustrated in Figs. 3 and 4 [3]. The symbol Γ denotes the Dancoff factor. The term $\overline{P_{e,F}^{iso}}$ represents the escape probability of neutrons from an isolated fuel rod, while $\overline{P_{e,F}}$ indicates the escape

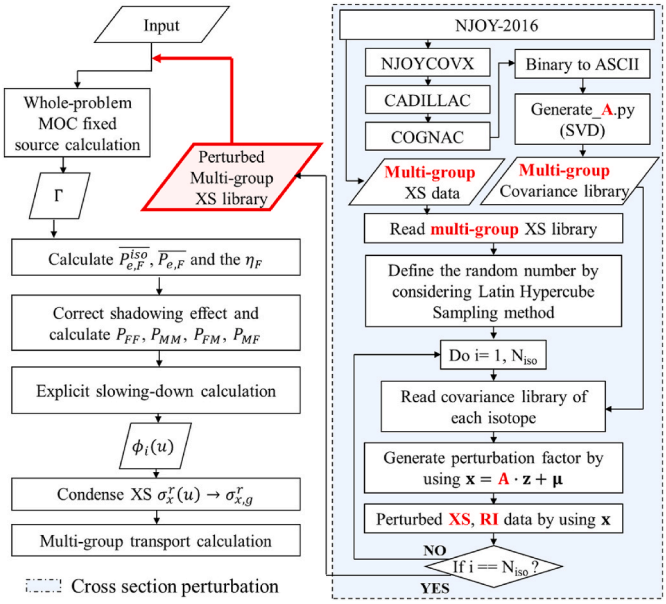

Fig. 4. Flowchart of perturbed XS based on EQ VCM.

probability from a fuel rod within a lattice; the overbar signifies a parameter calculated under the assumption of a single flat source region within the fuel pellet. The factor η_F adjusts for the shadowing effect. The probability of neutron collisions from one fuel region to another is expressed as P_{ij} for fuel-to-fuel interactions, P_{iM} for interactions from the fuel region to the moderator region, and P_{Mi} for the opposite. P_{MM} represents the probability of collisions within the non-fuel region. The flux in submesh i of the fuel rod is denoted by $\varphi_i(u)$. The term P^{iso}_{ij} refers to the first-flight collision probability from submesh i to j for an isolated fuel pin. Lastly, $\sigma^r_x(u)$ is the pointwise cross section, and $\sigma^r_{x,i,g}$ is the position-dependent multi-group cross section.

The more details of gray region of Fig. 2 is presented in those figures. The blue section represents the generation of the covariance library for PSM and EQ data. N denotes the number of samples. NJOY-2016 generates a covariance library as a COVFIL format file. NJOYCOVX converts a COVFIL file into a COVERX file [22,23]. CADLLAC and COGNAC were included in SCALE 6.1 code package [24]. CADILLAC combines multiple covariance data files into a single file. COGNAC converts COVERX-formatted libraries from BCD to binary format files. Before the SVD of the covariance matrix, the binary format files were converted to ASCII format data files because the Python script uses ASCII format data files. In this study, a total of 500 perturbed libraries are employed for the stochastic sampling method, as suggested by a prior study [25]. The STREAM code utilizes the covariance library to generate perturbed few-group constant data files (*.stn - STREAM to nodal). STORA (STREAM TO RAST-K), a linkage code, then converts these perturbed few-group constant data files into perturbed cross section data. Subsequently, RAST-K utilizes this perturbed cross section data to perform 3D core simulations. A notable distinction in the application between the EQ and PSM resonance treatments lies in the perturbation process within the STREAM calculations, which is influenced by covariance matrices generated by NJOY-2016. Particularly, the perturbation process in the resonance region exhibits differences between cases utilizing EQ and those employing PSM. Moreover, subsequent to the perturbation procedure, the fission spectrum underwent normalization, particularly in the interval between the perturbation phase and the transport calculation phase, as shown in Fig. 2. This normalization process was accomplished through the aggregation of the perturbed groupwise fission spectra.

Fig. 3 [3] presents two main components: the perturbation of the pointwise resonance intermediate (RI) library, covering a range from

Table 3
List of isotopes affected by ENDF/B-VII.1 VCM perturbation.

^{1} and ^{2}H	$^{28\text{-}29}$, and ^{30}Si	^{99}Tc	^{147}Pm	$^{229\text{-}230}$, ^{232}Pa
^{4}He	^{41}K	$^{101\text{-}104,106}$Ru	$^{149\text{-}151,152}$Sm	$^{230\text{-}233\text{-}234\text{-}235\text{-}236}$, ^{238}U
^{6} and ^{7}Li	$^{46\text{-}50}$Ti	^{103}Rh	^{153,155}Eu	$^{234\text{-}239}$Np
^{9}Be	$^{50\text{-}52}$, and ^{53}Cr	$^{105\text{-}108}$Pd	$^{152\text{-}160}$Gd	$^{236\text{-}240\text{-}241}$, $^{242\text{-}246}$Pu
^{10} and ^{11}B	^{55}Mn	^{109}Ag	$^{166\text{-}168,170}$Er	$^{240\text{-}241\text{-}242\text{-}}$ ^{242}m, ^{243}Am
C	$^{54\text{-}56}$, and ^{57}Fe	^{127,129}I	^{169}Tm	$^{240\text{-}250}$Cm
^{15}N	^{59}Co	$^{131\text{-}132,134}$Xe	$^{180\text{-}182\text{-}184}$, ^{186}W	$^{245\text{-}250}$Bk
^{16}O	^{58} and ^{60}Ni	^{133} and ^{135}Cs	^{191,193}Ir	$^{246, 248\text{-}254}$Cf
^{19}F	^{89}Y	^{139}La	^{197}Ag	$^{251\text{-}255, 254m}$Es
^{23}Na	$^{90\text{-}96}$Zr	^{141}Ce	$^{204,206\text{-}209}$Pb	^{255}Fm
^{24}Mg	^{95}Nb	^{141}Pr	^{209}Bi	
^{27}Al	$^{92, 94\text{-}100}$Mo	$^{143\text{-}145\text{-}146}$, and ^{148}Nd	$^{227\text{-}234}$Ac	

0.3 eV to 30 keV, and the perturbation of cross section data, spanning from 10^{-5} eV to 20 MeV. Perturbations are applied using 10,000 and 72 energy group structures for the RI and cross section libraries, respectively. To create the PSM library, modifications had been made to the ERRORR and GROUPR modules, specifically in terms of matrix size and memory size definitions. To assess the calculation capability of the modified NJOY-2016, a comparison is conducted using isotope uncertainty generated by the modified software. The PSM resonance treatment case utilizes covariance matrices **C** and $\mathbf{C_{PSM}}$, while matrices **A** and $\mathbf{A_{PSM}}$ are employed for cross section perturbation.

The perturbation method is derived from previous studies [21,26]. The covariance matrix was defined based on reactions presented in Tables 1 and 2: Equation (2) illustrates the covariance matrix for the 72 energy group structure, and Equation (3) represents the covariance matrices for the 10,000 energy group structures. Table 3 lists the 182 isotopes perturbed by covariance library.

$$\mathbf{C} = \begin{bmatrix} \Sigma_{R1,R1} & \cdots & \Sigma_{R1,R10} & \Sigma_{R1,R11} & \mathbf{O} & \mathbf{O} & \mathbf{O} \\ \vdots & \ddots & \vdots & \vdots & \vdots & \vdots & \vdots \\ \Sigma^T_{R1,R10} & \cdots & \Sigma_{R10,R10} & \Sigma_{R10,R11} & \mathbf{O} & \mathbf{O} & \mathbf{O} \\ \Sigma^T_{R1,R11} & \cdots & \Sigma^T_{R10,R11} & \Sigma_{R11,R11} & \mathbf{O} & \mathbf{O} & \mathbf{O} \\ \mathbf{O} & \cdots & \mathbf{O} & \mathbf{O} & \bar{\nu}_p & \mathbf{O} & \mathbf{O} \\ \mathbf{O} & \cdots & \mathbf{O} & \mathbf{O} & \mathbf{O} & \bar{\nu}_d & \mathbf{O} \\ \mathbf{O} & \cdots & \mathbf{O} & \mathbf{O} & \mathbf{O} & \mathbf{O} & \chi \end{bmatrix}, \tag{2}$$

$$\mathbf{C_{PSM}} = \begin{bmatrix} \Sigma_{R_{PSM}1,R_{PSM}1} & \Sigma_{R_{PSM}1,R_{PSM}2} & \Sigma_{R_{PSM}1,R_{PSM}3} \\ \Sigma^T_{R_{PSM}1,R_{PSM}2} & \Sigma_{R_{PSM}2,R_{PSM}2} & \Sigma_{R_{PSM}2,R_{PSM}3} \\ \Sigma^T_{R_{PSM}1,R_{PSM}3} & \Sigma^T_{R_{PSM}2,R_{PSM}3} & \Sigma_{R_{PSM}3,R_{PSM}3} \end{bmatrix}, \tag{3}$$

where **O** matrix contains the zeros, and size is 72 × 72. The notation of Σ_{I_1,I_2} is the covariance data, representing the interrelationship between the I_1 cross section and I_2 cross sections, is encapsulated within a matrix of dimensions 72 × 72. The structural designs of I_1 and I_2 are produced through the application of R_X, where the notation X denotes the reaction indices as outlined in Table 1. For instance, R_1 represents elastic scattering and R_2 denotes inelastic scattering. The notation R_{PSMX} corresponds to the reactions presented in Table 2. For instance, R_{PSM1} signifies a fission cross section. The matrix size of the terms in Equation (3) was 10,000 × 10,000.

Term represents the transposed matrix. The covariance matrix is decomposed via SVD as shown in Equation (4) [21]. Matrix **A**, utilized for the perturbation in STREAM, was calculated using Equation (5) [21].

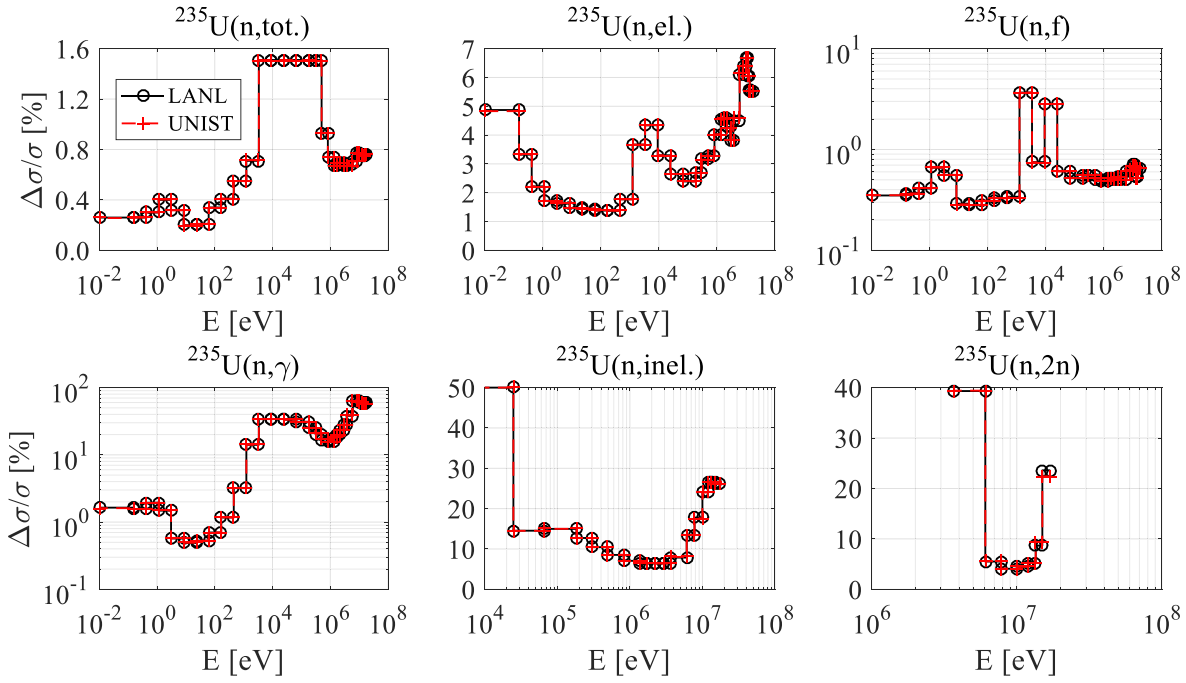

Fig. 5. XS uncertainty ($\Delta\sigma/\sigma$) of ^{235}U across different energy levels.

Matrix **A** is used in the neutron perturbation within STREAM. where $\mathbf{C_{psm}}$ denotes the covariance matrix used in the PSM resonance treatment. Equations (6) and (7) are applied to the PSM covariance library. The final equation forms are defined as Equations (8) and (9). These equations are used for perturbation of cross section in STREAM.

$$\mathbf{C} = \mathbf{U\Sigma U^T} = \mathbf{AA^T}, \tag{4}$$

$$\mathbf{A} = \mathbf{U}\sqrt{\mathbf{\Sigma}}, \tag{5}$$

$$\mathbf{C_{PSM}} = \mathbf{U_{PSM}\Sigma_{PSM}U_{PSM}^T} = \mathbf{A_{PSM}A_{PSM}^T}, \tag{6}$$

$$\mathbf{A_{PSM}} = \mathbf{U_{PSM}}\sqrt{\mathbf{\Sigma_{PSM}}}, \tag{7}$$

$$\mathbf{x} = \mathbf{A}\cdot\mathbf{z} + \boldsymbol{\mu}, \tag{8}$$

$$\mathbf{x} = \mathbf{A_{PSM}}\cdot\mathbf{z} + \boldsymbol{\mu}, \tag{9}$$

where $\mathbf{\Sigma}$, **U**, $\mathbf{\Sigma_{PSM}}$, and $\mathbf{U_{PSM}}$ are the results of SVD of the covariance matrices. A Python script was used for the SVD [26]. Matrices $\mathbf{\Sigma}$ and **U** are 72 × 72 matrices, and matrices $\mathbf{\Sigma_{PSM}}$ and $\mathbf{U_{PSM}}$ are 10,000 × 10,000 size matrices. Matrix **A** and $\mathbf{A_{PSM}}$ were used for perturbation in STREAM.

In addition, in order to mitigate the issue of negative XSs emerging throughout the perturbation procedure, a zero-cutoff strategy was implemented, consistent with methodologies delineated in prior UQ research [27,28]. Furthermore, the Latin Hypercube Sampling (LHS) technique was utilized for the generation of random numbers, a method validated by earlier investigations [29]. Random seeds were generated based on the Box-Muller transform, as shown in Equation (10) [29].

$$\begin{cases} r_1 = \sqrt{-2\,ln\,\alpha_1}sin(2\pi\alpha_2) \\ r_2 = \sqrt{-2\,ln\,\alpha_1}cos(2\pi\alpha_2) \end{cases}, \tag{10}$$

where r_1 and r_2 are random numbers following a normal distribution. The variables α_1 and α_2 represent random variables that adhere to a uniform distribution, spanning the interval from zero to one. To evaluate the covariance library generation process, as depicted in Fig. 2, LANL results were used for verification [30]. Fig. 5 shows the results of this comparison. The comparison results of the other isotopes are presented in Ref. [31]. For consistency in calculation conditions, a 33 energy group

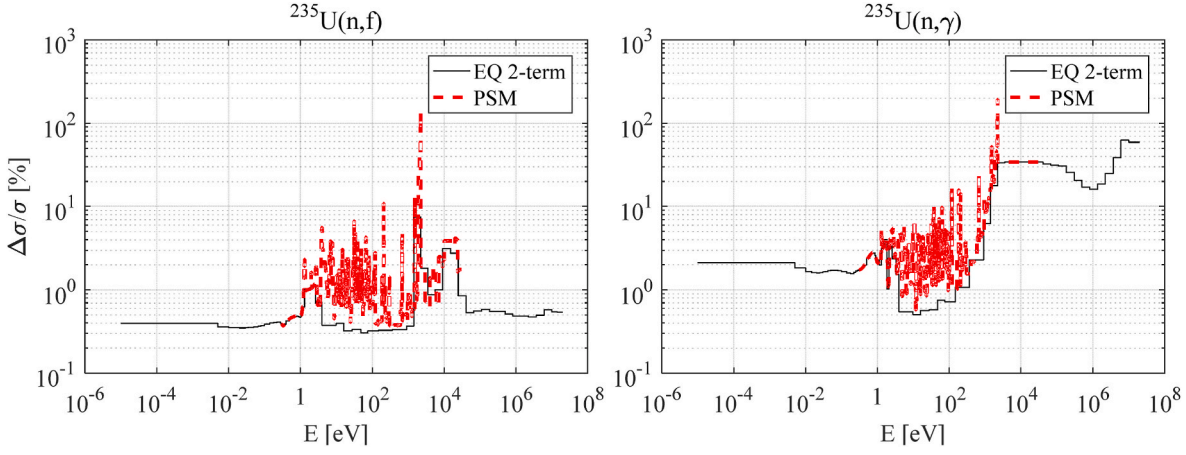

Fig. 6. Covariance library for EQ and PSM.

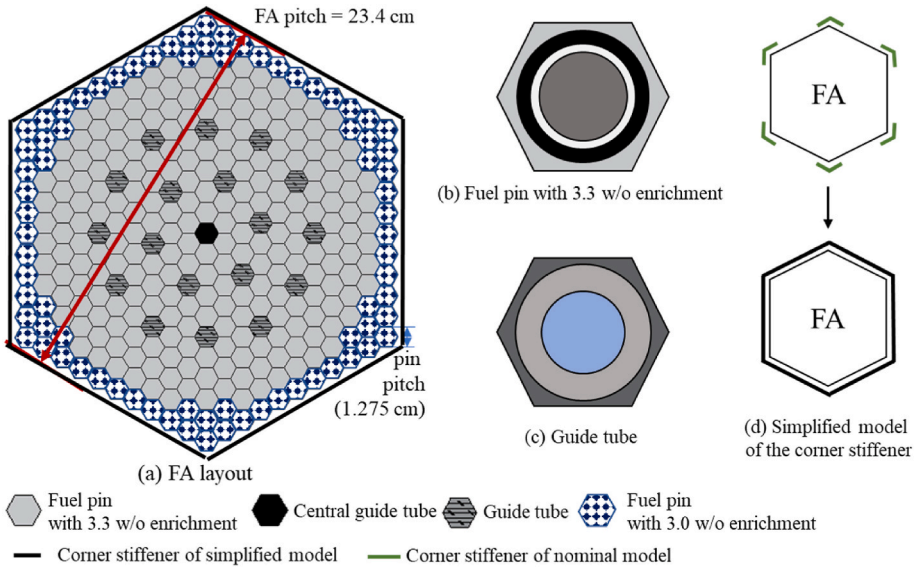

Fig. 7. Geometric arrangement of the Kozloduy-6 Fuel Assembly and the model of the pin cell.

Table 4
Specification of Kozloduy-6.

Content		Variable	Unit
Number of fuel rod		312	
Number of guide tube		18	
FA pitch		23.60	cm
Corner stiffener inner pitch [33]		23.35	cm
Outer radius	air gap	0.3860	cm
	Cladding	0.4550	cm
	Central guide tube	0.5600	cm
	Guide tube	0.6300	cm
Pin pitch		1.275	cm
Number of Instrument tube		1	
Fuel radius		0.3780	cm
Corner stiffener outer pitch [33]		23.48	cm
Inner radius	Central guide tube	0.4800	cm
	Guide tube	0.5500	cm
FA dimensions		11 × 11	

structure was used. Covariance data were generated based on ENDF/B-VII.1. Fig. 5 shows the cross sectional uncertainty ($\Delta\sigma/\ \sigma$) of ^{235}U. Isotopes were selected considering that they primarily contribute to the uncertainty for comparison. As indicated in this figure, the generated covariance library exhibits an accuracy comparable to that of the LANL. where (n, tot) represents the total XS, (n, inel) signifies the inelastic scattering XS, (n, f) denotes the fission XS, (n, γ) represents the capture XS, (n, 2n) indicates the production of deuterons, and (n, el) refers to the elastic scattering XS.

Fig. 6 displays the XS uncertainty derived from covariance libraries. Specifically, the EQ and PSM methods employ different covariance libraries in the resonance region, as depicted in the figures. The resonance region is defined as ranging from 0.3 eV to 30 keV. For the PSM calculation, the covariance library marked as 'PSM' in this figure is utilized. Furthermore, a 10,000 group energy structure is employed for the PSM calculation within the resonance treatment region.

3. Description of benchmark problems

The Kozloduy-6 benchmark problem was employed to evaluate the performance of a UQ module designed for hexagonal-geometry FAs [32]. Fig. 7 shows the detailed layouts. Subplot (b) illustrates the fuel pin layout, and subplot (c) shows the guide tube layout. Further details are presented in Table 4. The UAM benchmark document [7] does not provide specific information regarding corner stiffeners in fuel assemblies. Detailed information is obtained from the X2 document [33], which related to the VVER-1000 fuel assembly used in the X2 reactor was obtained from the X2 document [33]. This FA is similar to the Kozloduy-6 FA. Because the STREAM limitations do not accommodate the geometry presented in subplot (d) of Fig. 7, a simplified corner stiffener model was used in the calculations as a substitute for the nominal corner stiffener model.

A verification process using Serpent 2 [34] compared the calculation capacities of the simplified and nominal models. The calculations involved 48,000,000 neutrons, including 100 active cycles, 20 inactive cycles, and 400,000 histories per cycle. ENDF/B-VII.0 library [35] is utilized for computational purposes. The up-scattering correction for ^{238}U was not considered in this calculation [34]. The observed differences between the simplified and nominal models amount to 71 pcm, with a standard deviation of ±7 pcm, suggesting that the simplified calculation model has comparable accuracy to the nominal model. Therefore, a simplified calculation module is used in this study.

4. Results and discussion

This section outlines the computational outcomes for the Kozloduy-6 benchmark and delves into the validation findings of Kozloduy-6. The SCALE 6.2.2 code, which is widely used to analyze the uncertainty of neutronics data with the UAM benchmark [36–40], serves as the basis for comparative analysis between codes. During verification of the UQ module adapted in STREAM, TSUNAMI of SCALE 6.2.2 [41] was used. TSUNAMI calculates the uncertainties based on the GPT [4]. STREAM uses the stochastic sampling method with 500 perturbed cross sectional datasets.

Section 4.1 details the verification results of the UQ module, developed specifically for hexagonal-geometry FA, using SCALE 6.2.2. Section 4.2 encompasses the validation outcomes aimed at assessing the computational proficiency of the perturbation module and covariance libraries within the PSM approach.

4.1. Verification of UQ module for hexagonal geometry FA with SCALE 6.2.2

This section showcases the validation findings in comparison to the results acquired from SCALE 6.2.2. The Kozloduy-6 FA served as the verification model. For comparison, two separate cases from SCALE

Table 5
Temperature conditions for analysis of Kozloduy-6 benchmark.

Condition	HZP		HFP	
Parameter	Fuel	Moderator	Fuel	Moderator
Temperature [K]	552.15	552.15	900	560

6.2.2, 252-group (252G) and 56-group (56G), were used. The 252G and 56G cases employ the xs252v7.1, and xn56v7.1, neutronics libraries, respectively [4], both of which are rooted in the ENDF/B-VII.1 [5]. STREAM uses the 72G ENDF/B-VII.1 neutronics library. In this section, the SCALE 6.2 VCM is utilized. A 0.05 cm MOC ray was applied in the STREAM calculation. Two distinct operational scenarios were employed, specifically hot full power (HFP) and hot zero power (HZP). Boron concentration is defined as 0 ppm in this calculation. Detailed information is presented in Table 5.

Table 6 presents the calculation results for Kozloduy-6. Table 6 details the specific effects of the seven different reactions on the UQ calculation, total uncertainty of the multiplication factor and average of multiplication factors. Fig. 8 also includes the calculation results from SCALE 6.2.2 and STREAM. As demonstrated in the table and figure provided, STREAM demonstrates an accuracy comparable to that of SCALE 6.2.2. Specifically, the STREAM results align more closely with the 252G case from SCALE 6.2.2.

4.2. Verification of PSM VCM

This segment elaborates on the authentication of the newly integrated UQ module through the PSM VCM, as opposed to the EQ method. Because the EQ method has already been verified in Section 4.1, it is used here for a comparative analysis between codes. The ENDF/B-VII.1 VCM was used for the calculations. The average keffs and uncertainties of keff are presented in Table 7. Fig. 9 also contains the verification results of PSM method. As shown in these results, the PSM case has results comparable to of the EQ case. ENDF/B-VII.1 VCM and neutronics library are used for verification.

4.3. Verification of UQ module implemented in STREAM/RAST-V with Kozloduy-6

This section presents the calculation capability of developed UQ module during 3D core simulation using STREAM/RAST-V. Kozloduy-6 was used for verification. STREAM is used for comparisons as shown in Fig. 10. The multiplication factors and uncertainties are compared in

Table 7
$\overline{keff}$ and uncertainty (△k/k [%]) of Kozloduy-6 FA.

Condition	HZP		HFP	
1. $\overline{keff}$				
Method	EQ	PSM	EQ	PSM
$\overline{keff}$	1.32945	1.33075	1.31434	1.31612
2. Uncertainty (△k/k [%])				
Method	EQ	PSM	EQ	PSM
Reaction				
^{235}U (ν)	0.6202	0.6199	0.6186	0.6184
^{238}U (n, γ)	0.3297	0.3020	0.3416	0.3155
^{235}U (n, γ)	0.1717	0.1584	0.1716	0.1580
^{235}U (χ)	0.1407	0.1402	0.1454	0.1448
^{238}U (n, n')	0.1034	0.1029	0.1084	0.1078
^{235}U (n, f)	0.0969	0.0850	0.0967	0.0846
^{238}U (ν)	0.0692	0.0690	0.0707	0.0705
all	0.7979	0.7907	0.8017	0.7941

Table 6
Kozloduy-6 FA uncertainty (△k/k [%]) and $\overline{keff}$ with SCALE 6.2 VCM.

Condition	HZP			HFP		
Code	SCALE 6.2.2		STREAM	SCALE 6.2.2		STREAM
1. $\overline{keff}$						
Group	56G	252G	72G	56G	252G	72G
	1.32073	1.32414	1.32853	1.30844	1.31232	1.31341
2. Uncertainty (△k/k [%])						
Group	56G	252G	72G	56G	252G	72G
Reaction						
^{235}U (ν)	0.3516	0.3517	0.3511	0.3513	0.3514	0.3594
^{238}U (n, γ)	0.3169	0.3058	0.3054	0.3238	0.3111	0.3068
^{235}U (n, γ)	0.1732	0.1734	0.1759	0.1731	0.1732	0.1758
^{235}U (χ)	0.1485	0.1413	0.1362	0.1510	0.1437	0.1409
^{238}U (n, n')	0.1158	0.0990	0.0938	0.1159	0.0991	0.0937
^{235}U (n, f)	0.0936	0.0920	0.1022	0.0955	0.0939	0.1072
^{238}U (ν)	0.0654	0.0649	0.0692	0.0660	0.0655	0.0707
all	0.5745	0.5656	0.5814	0.5798	0.5697	0.5878

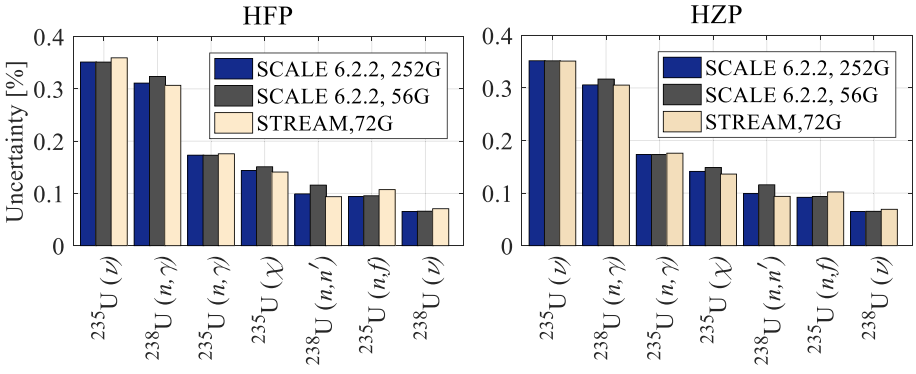

Fig. 8. Uncertainty of Kozloduy-6 with SCALE 6.2.2.

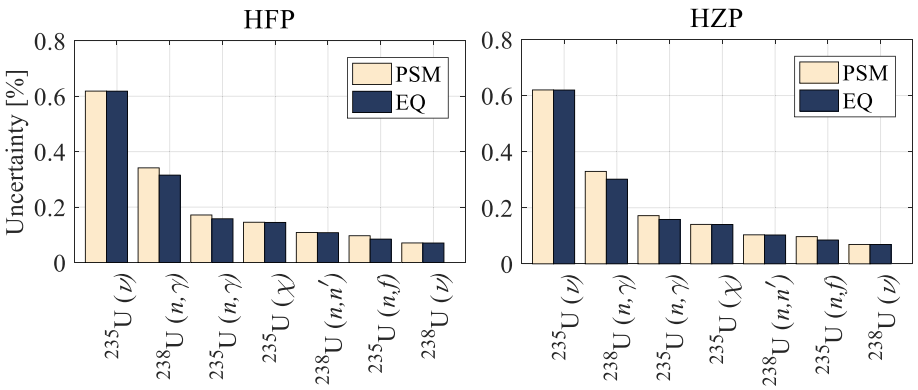

Fig. 9. Uncertainty analysis in relation to PSM and EQ resonance approaches.

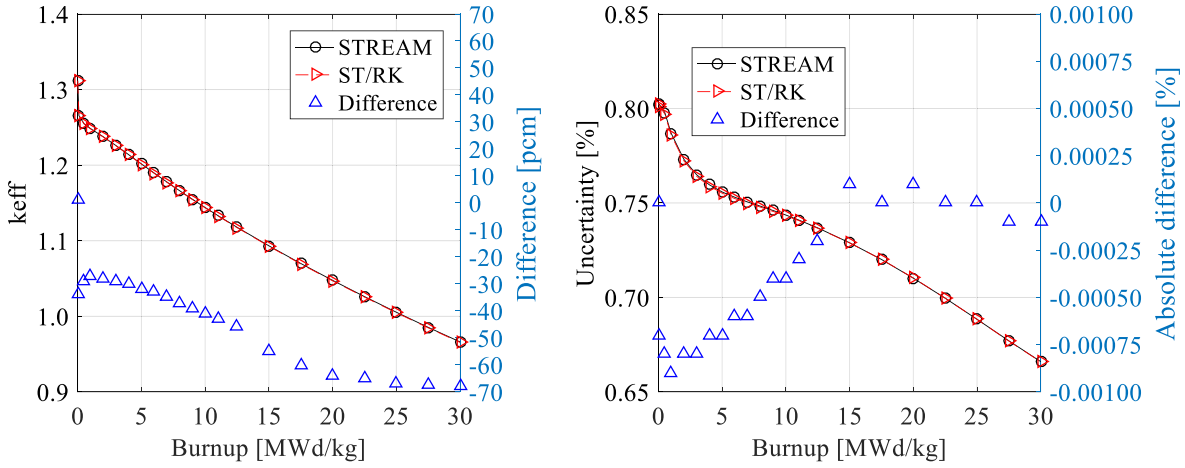

Fig. 10. Comparative Analysis of ST/RK results and STREAM results.

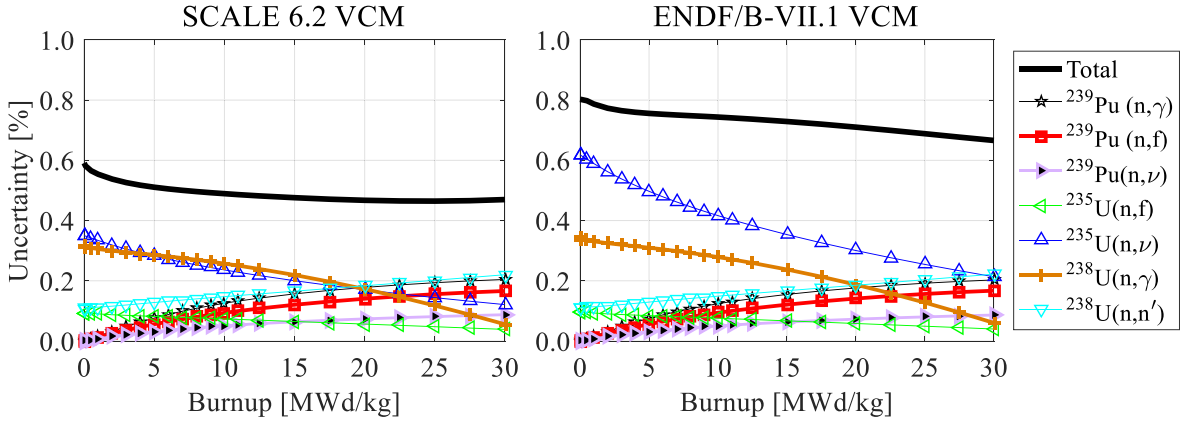

Fig. 11. Uncertainty analysis across burnup levels using SCALE 6.2 and ENDF/B-VII.1.

this figure, and the results provide an accuracy comparable to those obtained using STREAM. The calculation was performed using 500 perturbed samples under the following conditions at HFP condition. ENDF/B-VII.1 VCM and the EQ method were used for this calculation. These findings substantiate the fact that the STREAM/RAST-V two-step method delivers results with a precision comparable to that obtained from STREAM, confirming the reliability and effectiveness of the STREAM/RAST-V approach for uncertainty calculations.

Fig. 11 shows the uncertainty as a function of burnup for the principal effective reactions in UQ: capture, fission, and nu-bar of ^{239}Pu; fission, nu-bar, and capture of ^{235}U; and capture and inelastic scattering cross sections of ^{238}U. Two different covariance libraries were used for the calculation: SCALE 6.2 and ENDF/B-VII.1. It is important to note that the nu-bar of ^{235}U differs between the ENDF/B-VII.1 VCM and the SCALE 6.2 VCM case. As stated in the SCALE manual, the SCALE 6.2 VCM is derived from the ENDF/B-VII.2 preliminary library [42], whereas the ENDF/B-VII.1 VCM comes from the ENDF/B-VII.1 neutronics library. This discrepancy in the covariance libraries resulted in different uncertainties associated with the nu-bar of ^{235}U. The observed variations in the uncertainty of ^{235}U bar highlight the impact of the different covariance libraries on the calculated uncertainties. Therefore, it is crucial to consider these differences and their potential implications

when analyzing and interpreting the results.

5. Conclusion

For VVER analysis, this paper presents the UQ module developed in the STREAM/RAST-V two-step method. This study addresses two innovative calculation features: (1) generation of a library for PSM, and (2) development of a hexagonal-geometry FA analysis module. To evaluate the computational capability of the proposed scheme, the SCALE 6.2.2 and UAM benchmarks were used for comparison. Within the computational framework, the Kozloduy-6 benchmark serves as the basis. This analysis incorporates 500 perturbed instances, leveraging both ENDF/B-VII.1 neutronics data and the associated ENDF/B-VII.1 and SCALE 6.2 VCM.

Under both HZP and HFP conditions, the STREAM method achieves an accuracy comparable to that of SCALE 6.2.2. The differences are within ±0.0098% and ±0.0200% when compared with SCALE 6.2.2 using 56 and 256 energy group libraries, respectively. A PSM VCM was generated using NJOY-2016, CADILLAC, COGNAC, and NJOYCOVX. Compared to the UQ module for EQ, the developed PSM calculation module exhibits a difference within ±0.0076% in HZP and HFP FA model calculations, utilizing the ENDF/B-VII.1 VCM. Additionally, to assess the calculation capability of the STREAM/RAST-V two-step method in UQ analysis, verification is performed within a burnup range of 0–30 MWd/kg, with the uncertainty differences being within ±0.00100% between the two-step method and the lattice code STREAM.

Overall, this study provides a detailed description of the developed UQ module for VVER analysis and presents its verification. Future studies should encompass the implementation of UQ while considering its implicit effects.

Declaration of competing interest

There are no known conflicts of interest associated with this paper.

This work was supported by the National Research Foundation of Korea (NRF) grant funded by the Korea government (MSIT). (No. NRF-2019M2D2A1A03058371).

Acknowledgments

This work was supported by the National Research Foundation of Korea (NRF) grant funded by the Korea government (MSIT). (No. NRF-2019M2D2A1A03058371).

Abbreviations

252G	252-group
56G	56-group
72G	72-group
CRAM	Chebyshev rational approximation method
EQ	Calvik's two-term rational approximation
EQ 2-term	Calvik's two-term rational approximation
FA	fuel assembly
HFP	hot full power
HZP	hot zero power
PC	principal component
PSM	pin-based pointwise energy slowing down method
RI	resonance intermediate
SVD	singular value decomposition
UAM	uncertainty analysis in modeling
UQ	uncertainty quantification
VCM	variance-to-covariance matrix
XS	cross section

References

[1] J. Jang, C. Kong, B. Ebiwonjumi, Y. Jo, D. Lee, Uncertainties of PWR spent nuclear fuel isotope inventory for back-end cycle analysis with Stream/RAST-K, Ann. Nucl. Energy 158 (2021), https://doi.org/10.1016/j.anucene.2021.108267.

[2] J. Jang, C. Kong, B. Ebiwonjumi, A. Cherezov, Y. Jo, D. Lee, Uncertainty quantification in decay heat calculation of spent nuclear fuel by Stream/RAST-K, Nucl. Eng. Technol. 53 (2021) 2803–2815, https://doi.org/10.1016/j.net.2021.03.010.

[3] S. Choi, C. Lee, D. Lee, Resonance treatment using pin-based pointwise energy slowing-down method, J. Comp. Physiol. 330 (2017) 134–155, https://doi.org/10.1016/j.jcp.2016.11.007.

[4] B.T. Rearden, M.A. Jessee, SCALE Code System, Oak Ridge National Laboratory, 2017.

[5] M.B. Chadwick, M. Herman, P. Obložinský, M.E. Dunn, Y. Danon, A.C. Kahler, D. L. Smith, B. Pritychenko, G. Arbanas, R. Arcilla, R. Brewer, D.A. Brown, R. Capote, A.D. Carlson, Y.S. Cho, H. Derrien, K. Guber, G.M. Hale, S. Hoblit, S. Holloway, T. D. Johnson, T. Kawano, B.C. Kiedrowski, H. Kim, S. Kunieda, N.M. Larson, L. Leal, J.P. Lestone, R.C. Little, E.A. McCutchan, R.E. MacFarlane, M. MacInnes, C. M. Mattoon, R.D. McKnight, S.F. Mughabghab, G.P.A. Nobre, G. Palmiotti, A. Palumbo, M.T. Pigni, V.G. Pronyaev, R.O. Sayer, A.A. Sonzogni, N.C. Summers, P. Talou, I.J. Thompson, A. Trkov, R.L. Vogt, S.C. van der Marck, A. Wallner, M. C. White, D. Wiarda, P.G. Young, ENDF/B-VII.1 nuclear data for science and technology: cross sections, covariances, fission product yields and decay data, Nucl. Data Sheets 112 (2011) 2887–2996, https://doi.org/10.1016/j.nds.2011.11.002.

[6] D B, Kothe. CASL: The consortium for advanced simulation of light water reactors A DOE energy innovation hub. https://www.ne.anl.gov/mmsnf/presentations/Kothe.pdf, Oak Ridge National Laboratory.

[7] R.N. Bratton, M. Avramova, K. Ivanov, N. R, OECD/NEA benchmark for uncertainty analysis in modeling (UAM) for lwrs – summary and discussion of neutronics cases (phase I), Nucl. Eng. Technol. 46 (2014) 313–342, https://doi.org/10.5516/NET.01.2014.710.

[8] J. Jang, M. Hursin, W. Lee, A. Pautz, M. Papadionysiou, H. Ferroukhi, D. Lee, Analysis of Rostov-II benchmark using conventional two-step code systems, Energies 15 (2022) 3318, https://doi.org/10.3390/en15093318.

[9] J. Jang, S. Dzianisau, D. Lee, Development of nodal diffusion code RAST-V for Vodo–Vodyanoi Energetichesky reactor analysis, Nucl. Eng. Technol. 54 (2022) 3494–3515, https://doi.org/10.1016/j.net.2022.04.007.

[10] S. Choi, W. Kim, J. Choe, W. Lee, H. Kim, B. Ebiwonjumi, E. Jeong, K. Kim, D. Yun, H. Lee, D. Lee, Development of high-fidelity neutron transport code STREAM, Comput. Phys. Commun. 264 (2021), https://doi.org/10.1016/j.cpc.2021.107915.

[11] J. Park, J. Jang, H. Kim, J. Choe, D. Yun, P. Zhang, A. Cherezov, D. Lee, R.-K. Lee, RAST-K v2—three-dimensional nodal diffusion code for pressurized water reactor core analysis, Energies 13 (2020) 6324, https://doi.org/10.3390/en13236324.

[12] R.J.J. Stamm'ler, M.J. Abbate, Methods of Steady-State Reactor Physics in Nuclear Design, Academic Press Inc. (LONDON) LTD, 1983. ISBN 0-12-663320-7.

[13] D. Knott, A. Yamamoto, Lattice physics computations, in: D.G. Cacuci (Ed.), Handbook of Nuclear Engineering, Springer, 2010, pp. 913–1239.

[14] J. Jang, Development of Nodal Diffusion Code for VVER and HTGR Analysis with Advanced Semi Analytic Nodal Method, Ulsan National Institute of Science and Technology, 2023 doctoral thesis.

[15] D.W. Muir, R.M. Boicourt, A.C. Kahler, J.L. Conlin, W. Haeck, The NJOY Nuclear Data Processing System, Version 2016, LA-UR-17-20093, Los Alamos National Laboratory, 2016.

[16] J. Jang, B. Ebiwonjumi, W. Kim, A. Cherezov, J. Park, D. Lee, Verification and validation of isotope inventory prediction for back-end cycle management using two-step method, Nucl. Eng. Technol. 53 (2021) 2104–2125, https://doi.org/10.1016/j.net.2021.01.009.

[17] J. Jang, B. Ebiwonjumi, W. Kim, J. Park, J. Choe, D. Lee, Validation of spent nuclear fuel decay heat calculation by a two-step method, Nucl. Eng. Technol. 53 (2021) 44–60, https://doi.org/10.1016/j.net.2020.06.028.

[18] J. Choe, S. Choi, P. Zhang, J. Park, W. Kim, H.C. Shin, H.S. Lee, J. Jung, D. Lee, Verification and validation of Stream/RAST-K for PWR analysis, Nucl. Eng. Technol. 51 (2019) 356–368, https://doi.org/10.1016/j.net.2018.10.004.

[19] R.J.J. Stamm'ler, M.J. Abbate, Methods of Steady-State Reactor Physics in Nuclear Design, Academic Press Inc. (LONDON) LTD, 1983. ISBN 0-12-663320-7.

[20] D. Knott, A. Yamamoto, Lattice physics computations, in: D.G. Cacuci (Ed.), Handbook of Nuclear Engineering, Springer, US, Boston, Massachusetts, 2010, pp. 913–1239.

[21] A. Yamamoto, K. Kinoshita, T. Watanabe, T. Endo, Y. Kodama, Y. Ohoka, T. Ushio, H. Nagano, Uncertainty quantification of LWR core characteristics using random sampling method, Nucl. Sci. Eng. 181 (2015) 160–174, https://doi.org/10.13182/NSE14-152.

[22] G. Errorj, Chiba: A Code to Process Neutron-Nuclide Reaction Cross Section Covariance, Japan Atomic Energy Agency, 2007, version 2.3.

[23] K. Kosako, N. Yamano, Preparation of a covariance processing system for the evaluated nuclear data file, JENDL, (III),', Japan Nuclear Cycle De-Velopment Institute, 1999, pp. 1–114. JNC TJ 9440 99–003, vol.3, [in Japanese], https://jopss.jaea.go.jp/pdfdata/JNC-TJ9440-99-003.pdf.

[24] D. Wiarda, M.E. Dunn, N.M. Greene, M.L. Williams, C. Celik, L.M. Petrie, AMPX-6: a modular code system for processing ENDF/B, in: ORNL/TM-2016/43, Oak Ridge National Laboratory, 2016.

[25] G. Ilas, H. Liljenfeldt, Decay heat uncertainty for BWR used fuel due to modeling and nuclear data uncertainties, Nucl. Eng. Des. 319 (2017) 176e184, https://doi.org/10.1016/j.nucengdes.2017.05.009.

[26] V.C. Klema, A.J. Laub, The singular value decomposition: its computation and some applications, IEEE Trans. Automat. Control 25 (1980). https://ieeexplore.ieee.org/document/1102314.
[27] T. Zhu, Sampling-Based Nuclear Data Uncertainty Quantification for Continuous Energy Monte Carlo Codes, École Polytechnique Fédérale de Lausanne, 2015, https://doi.org/10.5075/epfl-thesis-6598.
[28] N.J. Quartemont, A.A. Bickley, J.E. Bevins, Nuclear data covariance analysis in radiation-trransport simulations utilizing SCALE sampler and the IRDFF nuclear data library, IEE, transactions on nuclear, Science 67 (2020) 482–491.
[29] K.A. Kinoshita, T. Yamamoto, Y. Endo, Y. Kodama, T. Ohoka, H. Ushio, Nagano. Uncertainty Quantification of Nutronics Characteristics Using Latin HyperCube Sampling Method, 2014. September 28, PHYSOR, Kyoto, Japan.
[30] R.E. MacFarlane, Covariance plots for ENDF/B-VII.1. https://t2.lanl.gov/nis/data/endf/covVII.1/, Los Alamos National Laboratory.
[31] J. Jang, Development of Nodal Diffusion Code for VVER and HTGR Analysis with Advanced Semi Analytic Nodal Method, Ulsan National Institute of Science and Technology, 2023 doctoral thesis.
[32] K.M. Ivanov, S. Avramova, I. Kamerow, E. Kodeli, E. Sartori, O. Ivanov, Cabellos., Benchmark for Uncertainty Analysis in Modelling (Uam) for Design, Operation and Safety Analysis of LWRs, I: Specification and Support Data for the Neutronics Cases (Phase I), OECD Nuclear Energy Agency, June 2016.
[33] Y. Bilodid, E. Fridman, T. Lötsch, X2 VVER-1000 benchmark revision: fresh HZP core state and the reference Monte Carlo solution, Ann. Nucl. Energy 144 (2020), https://doi.org/10.1016/j.anucene.2020.107558.
[34] J. Leppänen, M. Pusa, T. Viitanen, V. Valtavirta, T. Kaltiaisenaho, The Serpent Monte Carlo code: status, development and applications in 2013, Ann. Nucl. Energy 82 (2015) 142–150, https://doi.org/10.1016/j.anucene.2014.08.024.
[35] M.B. Chadwick, P. Obložinský, M. Herman, N.M. Greene, R.D. McKnight, D. L. Smith, P.G. Young, R.E. MacFarlane, G.M. Hale, S.C. Frankle, A.C. Kahler, T. Kawano, R.C. Little, D.G. Madland, P. Moller, R.D. Mosteller, P.R. Page, P. Talou, H. Trellue, M.C. White, W.B. Wilson, R. Arcilla, C.L. Dunford, S.F. Mughabghab, B. Pritychenko, D. Rochman, A.A. Sonzogni, C.R. Lubitz, T.H. Trumbull, J. P. Weinman, D.A. Brown, D.E. Cullen, D.P. Heinrichs, D.P. McNabb, H. Derrien, M. E. Dunn, N.M. Larson, L.C. Leal, A.D. Carlson, R.C. Block, J.B. Briggs, E.T. Cheng, H.C. Huria, M.L. Zerkle, K.S. Kozier, A. Courcelle, V. Pronyaev, S.C. van der Marck, ENDF/B-VII.0: next generation evaluated nuclear data library for nuclear science and technology, nuclear data sheets, next generation evaluated nuclear data library for nuclear science and technology, Nucl. Data Sheets 107 (2006) 2931–3060, https://doi.org/10.1016/j.nds.2006.11.001.
[36] E. Canuti, A. Petruzzi, F. D'Auria, T. Kozlowski, Sensitivity studies for the exercise I-1 of the OECD/UAM benchmark, Science and Technology of Nuclear Installations 2012 (2012) 10, https://doi.org/10.1155/2012/817185, 817185.
[37] H.J. Park, McCARD/MIG stochastic sampling calculations for nuclear cross section sensitivity and uncertainty analysis, Nucl. Eng. Technol. 54 (2022) 4272–4279, https://doi.org/10.1016/j.net.2022.06.012.
[38] A. Labarile, N. Olmo, R. Miró, T. Barrachina, G. Verdú, Comparison of SERPENT and SCALE methodology for LWRs transport calculations and additionally uncertainty analysis for cross section perturbation with SAMPLER module, EPJ Nuclear, Sci. Technol. 2 (2016), https://doi.org/10.1051/epjn/e2016-50002-7.
[39] L. Mercatali, K. Ivanov, V.H. Sanchez, SCALE modeling of selected neutronics test problems within the OECD UAM LWR's benchmark, Sci. Technol. Nucl. Installations. 2013 (2013) 1–11, https://doi.org/10.1155/2013/573697.
[40] C. Arenas, R. Bratton, F. Reventos, K. Ivanov, Uncertainty analysis of light water reactor fuel lattices, Sci. Technol. Nucl. Installations. 2013 (2013) 1–10, https://doi.org/10.1155/2013/437409.
[41] B.T. Rearden, M.L. Williams, M.A. Jessee, D.E. Mueller, D.A. Wiarda, Sensitivity and Uncertainty Analysis Capabilities and Data in SCALE, vol. 174, 2011, https://doi.org/10.13182/NT174-236.
[42] SCALE, A modular code system for performing standardized computer analyses licensing evaluation, NUREG/CR-0200, Rev.4 (ORNL/NUREG/CSD-2R4), Vols. and 111 (April 1995). RSIC code package CCC-545, version 4.2.